Mitigation of humaninduced vertical vibrations of footbridges through crowd flow control

Received ; | Revised ; | Accepted

DOI: xxx/xxxx

RESEARCH ARTICLE

Mitigation of human-induced vertical vibrations of footbridges through crowd flow control

Fiammetta Venuti*[1] | Anna Reggio[2]

[1]Department of Architecture and Design, Politecnico di Torino, Italy
[2]Department of Structural, Building and Geotechnical Engineering, Politecnico di Torino, Italy

Correspondence
*Fiammetta Venuti, Department of Architecture and Design, Politecnico di Torino, Italy. Email: fiammetta.venuti@polito.it

Summary

Due to their lightweight, slenderness and extremely low structural damping, footbridges are prone to human-induced vibrations. As a consequence, vibration mitigation strategies, mainly Tuned Mass Dampers, have been often implemented to reduce their dynamic response under pedestrian loading. In this study, a novel strategy towards the mitigation of human-induced vertical vibrations of footbridges is investigated: instead of acting on the structure, it is proposed to act on the source of excitation, realising what can be suitably defined as *crowd flow control*. Crowd flow control aims at altering the distribution of the crowd density and, as a consequence, of the walking velocity and step frequency. The dynamic loading exerted by the pedestrians is thus modified and the input energy transferred to the footbridge is reduced. Crowd flow control can be easily and quickly implemented via either permanent (e.g., benches or light poles) or temporary (e.g., Jersey barriers) obstacles located along the footbridge span, and is expected to be cheaper than competing vibration mitigation strategies. The study is carried out by means of numerical simulations. A microscopic model of crowd dynamics is used to generate pedestrian trajectories and velocities, whose corresponding force signals are built and then applied to the single-degree-of-freedom model of an ideal footbridge. The performance of the crowd flow control is investigated by considering different obstacles locations, by assessing effectiveness and robustness against variations in the pedestrian excitation and by establishing comparisons with a linear viscoelastic TMD. An interpretation of the results from an energy perspective is finally provided.

KEYWORDS:
human-induced vibration, footbridges, vibration mitigation, crowd flow control, crowd dynamics, energy balance

1 | INTRODUCTION

Footbridges are very often lightweight and slender structures with extremely low structural damping. For this reason, they are prone to vibrations under dynamic loadings, in particular under human-induced excitation. In the last fifteen years, an increasing number of cases has been reported where vibration mitigation strategies had to be implemented, before or after a footbridge opening, to mitigate excessive human-induced vibrations (e.g, [13, 15, 8, 34]).

A valuable interpretation of vibration mitigation is based on energy considerations. In accordance with the law of conservation of energy, when a structural system is dynamically excited, the input energy transmitted by the source of excitation enters the system and here converts into different energy forms: mechanical energy, i.e., kinetic energy and elastic strain energy, induced by the structural vibration, and dissipated energy, e.g., viscous damping energy, due to the presence of non-conservative forces. From an energy perspective, then, a proper vibration mitigation strategy entails the reduction of the mechanical energy of the vibrating structure. Two basic approaches are viable: either increasing the energy dissipation by introducing supplemental damping devices into the structure or reducing the amount of the input energy entering the structure [33].

Typical vibration mitigation strategies applied to footbridges falls into the first approach, such as viscous dampers [13] and friction dampers [25]. A similar purpose is accomplished by transferring most of the structural vibration energy to an attached Tuned Mass Damper (TMD), composed, in its simplest form, of an auxiliary mass-spring-dashpot passive system that dissipates the energy away by vibrating out of phase with the structural motion [21]. TMDs have been widely applied on bridges for the dynamic response control against wind-induced loads, primarily [33]. Successful applications on pedestrian bridges exist, wherein the TMD is used to mitigate either vertical or horizontal human-induced vibrations [13, 15, 5, 8, 10]. Unlike buildings, for which TMDs with high mass ratios have recently received considerable attention [14, 30], in bridges technical reasons cause the TMD mass to be typically below a few percent (1%-5%) of the structural mass. This limitation may possibly jeopardize, in practice, the effectiveness of the control device, as well as its robustness against the detuning effects derived from structural nonlinearities or uncertainties.

In this study, a novel strategy towards the mitigation of the human-induced vertical vibrations of footbridges is investigated: instead of acting on the structure, it is proposed to act on the source of excitation, realising what can suitably defined an excitation-based mitigation strategy. Examples of excitation-based mitigation strategies have been already implemented on tall buildings [23] or long-span bridges [31] to reduce wind-induced vibrations, through the shaping of the overall structure (e.g., elicoidal shape of tall buildings) or the introduction of punctual elements (e.g., guide vanes around bridge decks). When dealing with human-induced vibrations on footbridges, excitation-based mitigation strategies can be obtained via *crowd flow control*. Crowd flow control aims at altering the distribution of the crowd density and, as a consequence, of the walking velocity and step frequency, thus modifying the dynamic loading exerted by the pedestrians. Crowd flow control apparently falls into the second approach to vibration mitigation, since it modifies the characteristics of the pedestrian excitation in order to reduce the input energy transferred to the footbridge.

First suggested by Carroll et al. [9] and subsequently investigated by Venuti and Bruno [38] with reference to the smooth widening/narrowing of the walkway width along the footbridge span, crowd flow control has been applied, in both studies, only to the lateral vibrations due to Synchonous Lateral Excitation. In the present paper, crowd flow control is proposed for the mitigation of human-induced vertical vibrations and is achieved by means of obstacles located along the footbridge span. The idea comes from the fields of applied mathematics and transportation engineering, in which the problem of forcing the crowd flow to follow established patterns, e.g., in evacuation scenarios, is often solved through punctual blocks placed in strategic positions [18, 19]. The obstacles located along the footbridge span can be intended either as a permanent (e.g., benches or light poles) or as an emergency temporary measure (e.g., Jersey barriers). In the second case, they can be easily and quickly installed whenever the footbridge is expected to be crossed by a crowd density which could induce vibrations above the comfort limits. Further advantages can be envisaged: the design, installation and maintenance costs of the crowd flow control are foreseen to be lower than those of competing vibration mitigation strategies; a great flexibility is possible, because different obstacle locations can be adopted on the basis of the different traffic scenarios.

The paper develops as follows. Section 2 presents the adopted modelling approach. Section 3 is devoted to the design of the crowd flow control. In Section 4, a case study is set for the performance assessment of the crowd flow control; in order to emphasise similarities and differences with mitigation strategies well established in the engineering practice, comparisons with an optimally designed linear viscoelastic TMD are also provided. The results of the numerical investigations are illustrated and discussed in Section 5. Section 6 provides a deeper insight into the principle of operation of the crowd flow control from an energy perspective. Finally, in Section 7, conclusions and research perspectives are outlined.

2 | MODELLING APPROACH

The study is carried out on the basis of the following modelling assumptions:

a1. even though it is widely accepted that Human-Structure-Interaction (HSI) occurs when pedestrians walk on a flexible structure and a great number of studies have been recently devoted to this issue (e.g., [39], [26], [32],[17]), there is still great uncertainty about how to model HSI. Therefore, HSI is neglected in this study. This choice is justified by two main reasons: on the one hand, this allows it to better focus on the effects of the crowd flow on the structural response, without introducing further sources of uncertainty; on the other hand, modelling HSI still belongs to the research field, while codes and guidelines neglect its effects;

a2. the obstacles placed along the footbridge span to achieve the crowd flow control are modelled as purely geometrical constraints, not affecting the structural mass, stiffness and damping properties.

The adopted modelling approach is illustrated in Figure 1 and described below.

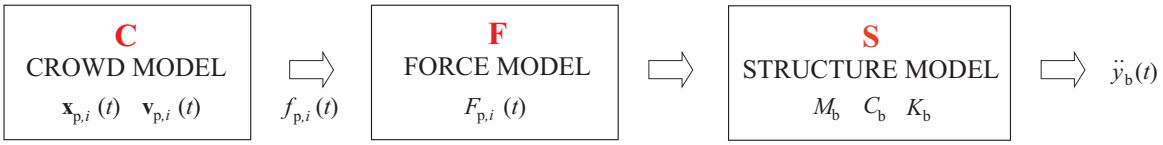

FIGURE 1 Scheme of the modelling approach

2.1 | Crowd model

Simulations of the crowd flow are performed through the software Mass Motion (MM) v. 8.5 [2], which is based on a microscopic model of the crowd dynamics derived, as a modified version, from the Social Force Model first proposed by Helbing and Molnár [20]. In such a model, each individual pedestrian is described as an agent, whose goal is to reach her final destination walking at her desired velocity. Desired velocities v_{des} are randomly assigned to the pedestrians from a Normal distribution, with mean 1.34 m/s and standard deviation (std) 0.26 m/s [6]. While walking, each agent is subjected to a set of forces that modify her desired velocity on the basis of the interaction with neighbouring pedestrians and the environment (walls, obstacles, etc.). The interested reader is referred to [20] and [2] for a detailed description of the mathematical and numerical framework.

Crowd flow simulations result in trajectory $\mathbf{x}_{p,i}(t) = [x_{p,i}, z_{p,i}]$ and velocity $\mathbf{v}_{p,i}(t) = [v_{xp,i}, v_{zp,i}]$ for each i-th pedestrian along time t, where x and z are the longitudinal and transverse axes of the footbridge, respectively.

2.2 | Force model

Trajectory $\mathbf{x}_{p,i}(t)$ and velocity $\mathbf{v}_{p,i}(t)$ are then used to build the moving time-varying force $F_{p,i}(t)$ exerted by the i-th pedestrian on the footbridge.

In the last fifteen years a great number of studies have been devoted to the experimental characterisation of pedestrian dynamic loading (e.g. [29, 24, 16, 22, 4]) and to the proposal of suitable human-induced load models of both single pedestrians and crowds (e.g. [29, 37, 28, 27, 12, 11]). In the framework of a comparative study, the classic continuous force model [3] is assumed, where $F_{p,i}(t)$ is described by a sum of n Fourier harmonic components:

$$F_{p,i} = G_{p,i} + \sum_{j=1}^{n} G_{p,i}\, DLF_j \sin(2\pi j f_{p,i}\, t - \theta_j), \tag{1}$$

where: $G_{p,i} = m_{p,i}\, g$ is the pedestrian weight, being $m_{p,i}$ the pedestrian mass and g the gravity acceleration; $f_{p,i}$ is the pedestrian step frequency; DLF_j and θ_j are, respectively, the Dynamic Load Factor and phase shift of the j-th contributing harmonic. Mass $m_{p,i}$ is randomly assigned to each pedestrian from a Normal distribution with mean 75 kg and std 15 kg [42]. DLF_j are expressed as functions of $f_{p,i}$, according to Young [41].

In this study, the pedestrian step frequency $f_{p,i}$ is considered as not constant in time and it is calculated as a function of the walking velocity $v_{p,i}(t)$, as proposed by Venuti and Bruno [36]:

$$f_{p,i}(t) = 2.93 v_{p,i}(t) - 1.59 v_{p,i}^2(t) + 0.35 v_{p,i}^3(t). \tag{2}$$

Note that the modifications introduced in the classic continuous force model allow to account for both inter-subject and intra-subject variability of human load.

2.3 | Structure model

The footbridge is modelled as a Single Degree of Freedom (SDOF) system, representing one structural vertical vibration mode of interest, whose dynamics is governed by the well-known equation of motion:

$$M_{\mathrm{b}}\ddot{y}_{\mathrm{b}} + C_{\mathrm{b}}\dot{y}_{b} + K_{\mathrm{b}}y_{\mathrm{b}} = F, \tag{3}$$

where: $y_{\mathrm{b}}(t)$ is the displacement response at the antinode, the overdot indicating differentiation with respect to time t; M_{b}, C_{b} and K_{b} are the modal mass, damping and stiffness of the footbridge, respectively; $F(t) = \sum_{i=1}^{N} F_{\mathrm{p},i}(t)\,\Phi\left(x_{\mathrm{p},i}(t)\right)$ is the modal force, being N the number of pedestrians walking on the footbridge at time t and $\Phi(x)$ the unity-normalised modal shape of the structure.

3 | DESIGN OF CROWD FLOW CONTROL

The proposed strategy of crowd flow control is based on the location of obstacles along the footbridge path. The expected effect is to induce variations in the pedestrian trajectories and velocities, thus modifying the dynamic force exerted on the footbridge, according to Equations 2, 4 and 1.

Two different types of obstacle location are considered (Figure 2):

- obstacles located on the footbridge longitudinal axis, in order to force Lane Separation (LS);
- obstacles located on the footbridge lateral edges, in order to obtain a Bottle Neck (BN), i.e. a local narrowing of the footbridge width.

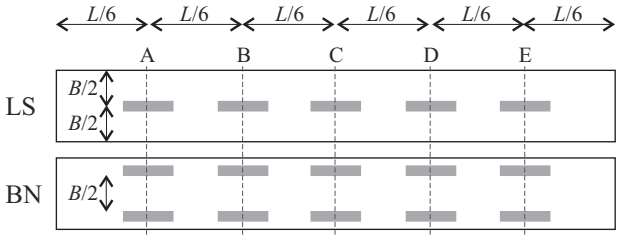

FIGURE 2 Scheme of the obstacle locations

In Table 1 , a list of the investigated controlled layouts is reported, with the indication of the number and position of the obstacles. For each obstacle, dimensions $l = L/10$ and $b = B/10$ have been assumed, being L and B the footbridge length and width, respectively.

4 | CASE STUDY

4.1 | Ideal footbridge

Numerical investigations are carried out on an ideal footbridge, sketched in Figure 3 . Its dimensional and dynamic properties are summarised in Table 2 , where m_{b}, f_{b} and ζ_{b} are mass per unit length, fundamental frequency and damping ratio, respectively. Frequency f_{b} and damping ratio ζ_{b} refers to the first symmetric vertical mode of the footbridge, for which a sinusoidal modal shape function $\Phi(x) = \sin(\pi x/L)$ is assumed. Frequency f_{b}, in particular, is chosen within the range corresponding to the maximum risk of resonance according to the Setra guideline [1]. Consequently, only the first contributing harmonic of the

TABLE 1 Footbridge with crowd flow control, list of the investigated layouts

Footbridge layout	Type	N° of obstacles	Position of obstacles
L1	LS	1	C
L2	LS	3	B-C-D
L3	LS	5	A-B-C-D-E
L4	LS	2	B-C
L5	LS	2	B-D
L6	BN	2	C
L7	BN	6	B-C-D
L8	BN	10	A-B-C-D-E
L9	BN	6	A-C-E
L10	BN	6	A-B-C

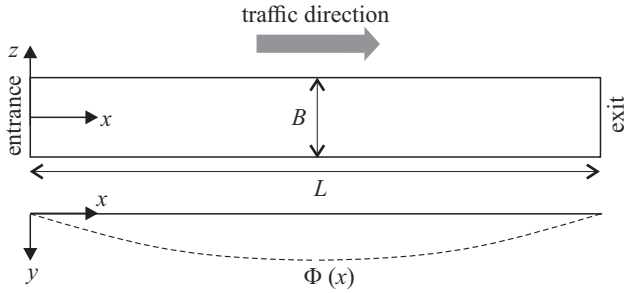

FIGURE 3 Schematic plan and side view of the footbridge

TABLE 2 Properties of the ideal footbridge

L [m]	B [m]	m_b [kg/m]	f_b [Hz]	ω_b [rad/s]	ζ_b [-]
100	3	1500	1.8	11.31	0.005

pedestrian load is taken into account in Equation 1, since the higher harmonics are expected to have a negligible influence on the structural response. The corresponding DLF_1 is expressed as [41]

$$DLF_1(t) = 0.41(f_{p,i}(t) - 0.95) \leq 0.56. \tag{4}$$

4.2 | Pedestrian traffic scenarios

Simulations of the crowd flow are performed under different pedestrian traffic scenarios, corresponding to mean crowd densities ρ_m on the footbridge in the range [0.1, 1] ped/m^2.

It has to be observed that, in the software MM used for the crowd dynamics simulations, boundary conditions at the footbridge entrance section can be set in terms of the total number of pedestrians N_{tot} entering the footbridge over a time T, with arrival times randomly generated according to a uniform distribution. Time T is taken as equal to 10 times the mean crossing time $T_m = L/v_m$, being v_m the mean walking velocity of the pedestrians. Such a long time interval is chosen to allow almost steady state traffic condition to develop, for which N_{tot} can be calculated as $10\rho_m LB$.

According to the above relations, a certain value of ρ_m can be obtained only if time T is correctly estimated, and this in turn depends on a correct estimate of v_m, which is not *a priori* known. Therefore, a preliminary parametric analysis has been carried out to properly tune time T.

A first set of ten simulations - one for each value of ρ_m in the considered range - has been performed, where v_m has been estimated as a function of ρ_m according to the Weidmann (W) fundamental law [6]:

$$v_{m,W} = 1.34 \left\{ 1 - \exp\left[-1.913 \left(\frac{1}{\rho_m} - \frac{1}{5.4} \right) \right] \right\}. \tag{5}$$

For each simulation, both mean crowd density ρ_m and mean walking velocity v_m have been calculated over a time interval T_{full} corresponding to the full occupancy of the footbridge. The latter has been derived by excluding the initial and final durations in which the pedestrians populate and leave the bridge, respectively. The lower and upper boundaries of T_{full} have been determined as the first and last time instant when a mean number of pedestrians N_m are on the footbridge, being $N_m = \rho_m LB$.

Results are reported in Figure 4 (a). The mean walking velocities obtained from the numerical simulations (black circles) are lower than those predicted through Eq. 5, and consequently the mean crowd densities are different than expected. Therefore, a second run was necessary to tune time T in order to obtain the expected average density on the footbridge (white circles).

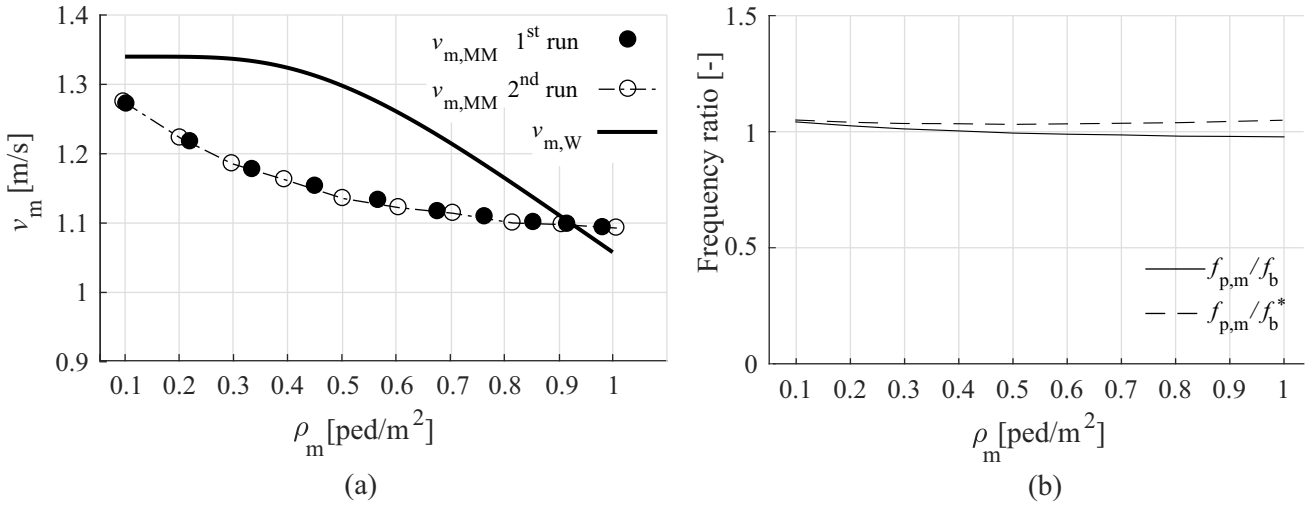

FIGURE 4 Mean walking velocity v_m (a) and frequency ratio (b) vs mean crowd density ρ_m.

Figure 4 (b) plots the ratio between the mean step frequency $f_{p,m}$ and the footbridge natural frequency f_b in solid line. The mass of the pedestrians can cause a significant increase in the footbridge modal mass in case of high pedestrian to bridge mass ratio and a consequent modification of the footbridge frequency. To quantify this effect, the modified footbridge frequency f_b^*, which accounts for the pedestrian added mass, is calculated and the ratio $f_{p,m}/f_b^*$ is plotted in dashed line. It can be observed that the difference between the two curves is negligible (below 7%) and that the solid line is generally closer to the unit value, which is the worst case scenario. For these reasons, the contribution of the pedestrian added mass has been neglected. This is in agreement with assumption a1 and is expected not to affect the results of a comparative study.

4.3 | Design of TMD

The case of a linear viscoelastic TMD controlling the dynamic response of the footbridge is considered for comparison purposes.

The TMD is tuned to the first symmetric vertical mode of the footbridge and is connected to it at the mid-span section, i.e., where the relevant modal shape function $\Phi(x)$ attains its maximum value. Setting this value to unity, or $\Phi(L/2) = 1$, a

generalised SDOF structure–TMD system can be introduced (Figure 5), whose equations of motion are given as

$$M_{\mathrm{b}}\ddot{y}_{\mathrm{b}} + C_{\mathrm{b}}\dot{y}_{b} + K_{\mathrm{b}}y_{\mathrm{b}} = F + u, \tag{6a}$$

$$m_{\mathrm{d}}\ddot{y}_{\mathrm{d}} = -u, \tag{6b}$$

$$u = c_{\mathrm{d}}(\dot{y}_{\mathrm{d}} - \dot{y}_{\mathrm{b}}) + k_{\mathrm{d}}(y_{\mathrm{d}} - y_{\mathrm{b}}), \tag{6c}$$

in which: $y_{\mathrm{b}}(t)$, M_{b}, C_{b}, K_{b} and $F(t)$ have been defined in Section 2.3; $y_{\mathrm{d}}(t)$ is the TMD displacement; m_{d}, c_{d} and k_{d} are, respectively, the mass, viscous damping constant and stiffness coefficient of the TMD; $u(t)$ is the force exerted by the TMD on the footbridge.

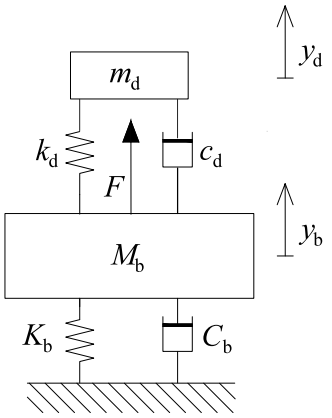

FIGURE 5 Structural model of the generalised SDOF structure–TMD system.

Equations 6 can be conveniently rewritten as

$$\ddot{y}_{\mathrm{b}} + 2\zeta_{\mathrm{b}}\omega_{\mathrm{b}}\dot{y}_{\mathrm{b}} + \omega_{\mathrm{b}}^2 y_{\mathrm{b}} = \frac{F}{M_{\mathrm{b}}} + \frac{u}{M_{\mathrm{b}}}, \tag{7a}$$

$$\mu\ddot{y}_{\mathrm{d}} = -\frac{u}{M_{\mathrm{b}}}, \tag{7b}$$

$$\frac{u}{M_{\mathrm{b}}} = 2\zeta_{\mathrm{d}}\alpha\omega_{\mathrm{b}}\mu\,(\dot{y}_{\mathrm{d}} - \dot{y}_{\mathrm{b}}) + \alpha^2\omega_{\mathrm{b}}^2\mu\,(y_{\mathrm{d}} - y_{\mathrm{b}}), \tag{7c}$$

to highlight the five parameters that govern the dynamic response of the generalised SDOF structure–TMD system: ω_{b} and ζ_{b} are the uncoupled modal frequency and damping ratio of the structure; $\zeta_{\mathrm{d}} = c_d/(2\sqrt{k_d\, m_d})$ is the uncoupled damping ratio of the TMD; $\mu = m_{\mathrm{d}}/M_{\mathrm{b}}$ and $\alpha = \omega_{\mathrm{d}}/\omega_{\mathrm{b}}$ are the mass ratio and frequency ratio of the system, denoting with $\omega_{\mathrm{d}} = \sqrt{k_{\mathrm{d}}/m_{\mathrm{d}}}$ the uncoupled natural frequency of the TMD. Within this set of parameters, $\omega_{\mathrm{b}} = 11.31$ rad/s and $\zeta_{\mathrm{b}} = 0.005$ are known from the dynamic properties of the footbridge (Table 1), mass ratio $\mu = 0.01$ is set out as a customary value in pedestrian bridges, frequency ratio α and damping ratio ζ_{d} have to be designed on the basis of an optimum criterion. In accordance with Warburton [40], who optimised the TMD by minimising the variance of the structural displacement under a random white noise force, the optimal values of the TMD design parameters are determined as

$$\alpha_{\mathrm{opt}} = \frac{\sqrt{1 + \frac{\mu}{2}}}{1 + \mu} = 0.9926, \tag{8a}$$

$$\zeta_{\mathrm{opt}} = \sqrt{\frac{\mu(1 + \frac{3}{4}\mu)}{4(1 + \frac{\mu}{2})(1 + \mu)}} = 0.0498. \tag{8b}$$

The applicability of the Warburton criterion to the case under consideration may be questioned, observing that: on the one hand, pedestrian traffic is not accurately represented by a white noise input; on the other hand, the minimisation of the displacement

response may not be a suitable optimisation criterion when the acceleration response is of concern. Recent numerical investigations conducted by Tubino and Piccardo [35] have demonstrated, however, that the Warburton criterion leads to a TMD control performance comparable to the one obtained by minimising the structural acceleration under unrestricted pedestrian traffic.

5 | PERFORMANCE OF CROWD FLOW CONTROL

In this Section, the results of the numerical investigations performed on the ideal footbridge are presented and discussed. In particular, comparisons are drawn among different footbridge layouts:

- the uncontrolled layout, denominated as L0;
- the footbridge with the crowd flow control implemented (layouts L1–L10)
- the footbridge with the TMD installed (layout L11).

For each layout and each value of the mean crowd density ρ_m, 20 simulations of the crowd dynamics were performed and the resulting acceleration time histories of the footbridge were obtained. The statistical reliability was checked by calculating mean and std of crowd density, walking velocity and peak acceleration during T_{full} and averaging their values over an increasing number of simulations. As an example, Figure 6 plots the relative error in the average estimation between successive simulations n and $n+1$ for L0 and $\rho_m = 0.4$ ped/m^2. The relative error falls below 1% for all the computed statistics and this level of accuracy is fully satisfactory for the present study.

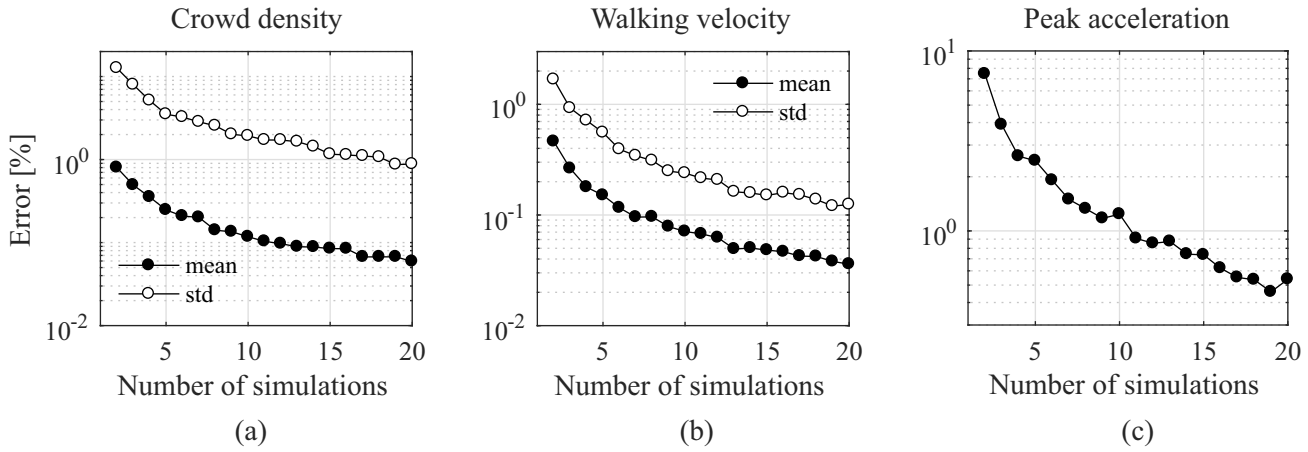

FIGURE 6 Relative error in the average estimation between successive simulations of (a) mean and std crowd density, (b) mean and std walking velocity and (c) peak acceleration

5.1 | Uncontrolled layout

Figure 7 illustrates an example of time histories of the number of pedestrians/crowd density on the footbridge and of the acceleration response for three values of crowd density: $\rho_m = 0.1$, 0.4 and 1 ped/m^2. The intermediate value has been chosen as the traffic condition corresponding to the frequency ratio f_r closest to unit in L0 (see Fig. 4). The Setra [1] acceleration limits that identify maximum, mean and minimum comfort regimes are reported as dashed lines in the acceleration time history plots. The response increases for increasing crowd density. Note that this is a consequence of having neglected the added damping effect induced by human-structure interaction [26] and a different trend could occur if HSI is taken into account. For $\rho_m = 0.1$ ped/m^2 (Fig. 7 a) the peak acceleration exceeds the lower limit of mean comfort, while for higher densities (Fig. 7 b,c) the peak response falls within the minimum comfort range.

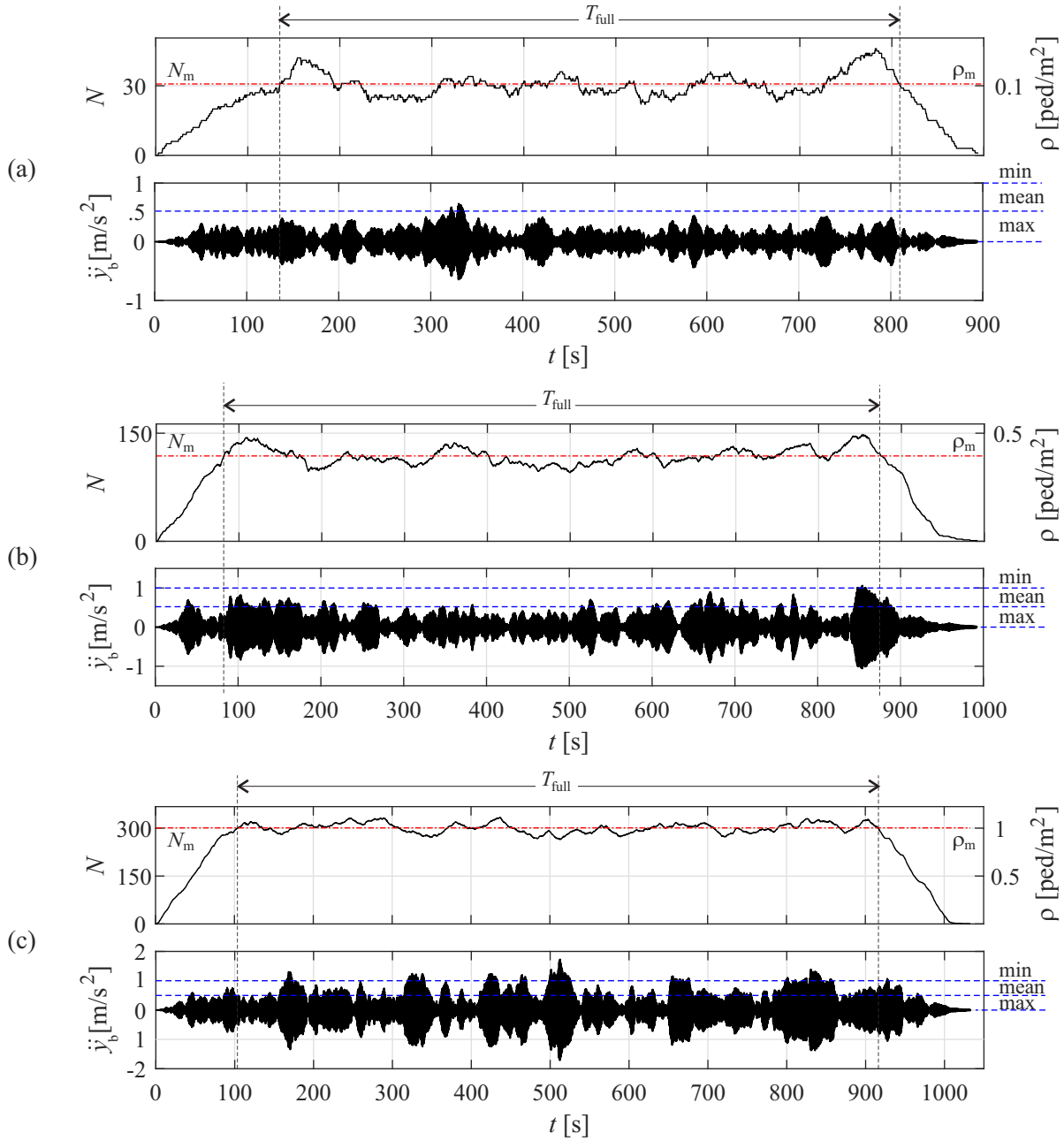

FIGURE 7 Example of time histories of the number of pedestrians N, pedestrian density ρ and acceleration response $\ddot{y}_b$ for (a) $\rho_m = 0.1$ ped/m^2, (b) $\rho_m = 0.4$ ped/m^2 and (c) $\rho_m = 1$ ped/m^2

Figure 8 a plots the probability density functions (PDF) of moduli v of actual velocity and v_{des} of desired velocity, as obtained with MM considering all the 20 simulations. It can be observed that the distribution of actual velocities follows a normal distribution as well as the desired velocities, but with lower mean and std. In particular, mean and std values decreases as the crowd density increases. This is expected, since desired velocities correspond to unconstrained pedestrian behaviour (i.e., a pedestrian walking alone, that is, ρ=0), while, in the presence of a higher crowd density, mean walking velocity decreases and std decreases as well. Step frequencies, calculated as a function of walking velocities, follow the same trend, in line with experimental observations [7] (Figure 8 b).

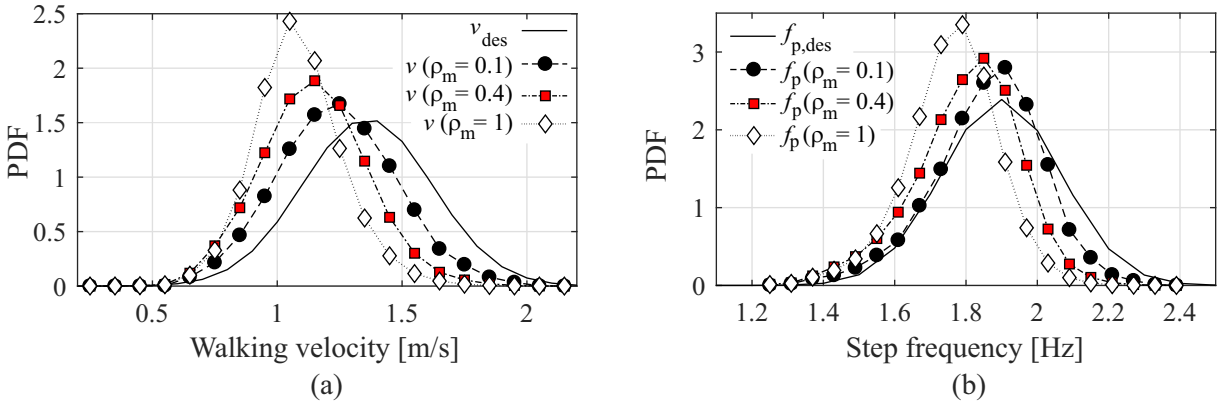

FIGURE 8 PDF of (a) desired walking velocities v_{des} and actual velocities v and (b) desired step frequencies $f_{\text{p,des}}$ and actual step frequencies f_p for $\rho_{\text{m}} = 0.1$, 0.4 and 1 ped/m^2

5.2 | Controlled layouts

With the aim of assessing the effectiveness and robustness of the crowd flow control, a performance index is defined as

$$r_{a,j} = a_{\text{peak},j}/a_{\text{peak},0} \quad \text{for } j = 1, 3, \ldots, 11, \tag{9}$$

where $a_{\text{peak},j}$ is the average peak acceleration of the footbridge in the j-th controlled layout, while $a_{\text{peak},0}$ is the average peak acceleration in the uncontrolled layout L0. For each layout, the average peak acceleration is computed by averaging the peak values of the 20 simulated acceleration time histories. Note that a value of $r_{a,j}$ smaller than one implies the effectiveness of the control strategy in reducing the footbridge acceleration response.

The values obtained for the performance index in each one of the controlled layouts, assuming three different values of the mean crowd density $\rho_{\text{m}} = 0.1$, 0.4 and 1 ped/m^2, are shown in Figures 9 -11 . As a reference, the Setra [1] acceleration limits, normalised with respect to $a_{\text{peak},0}$, are also reported as dash-dot horizontal lines.

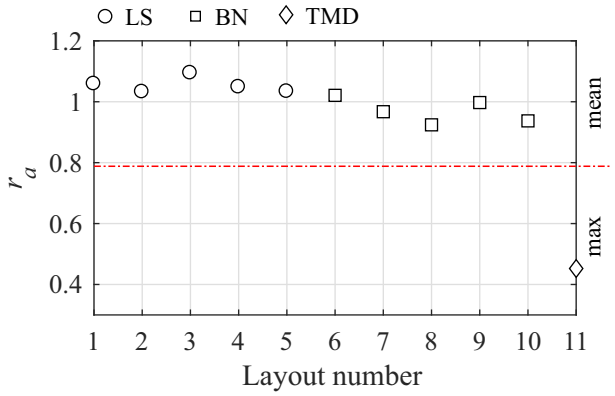

FIGURE 9 Performance index for each controlled layout, $\rho_{\text{m}} = 0.1$ ped/m^2

Regarding the crowd flow control, BN location is, in general, more effective than the LS one in reducing the peak acceleration response. This difference can be explained by looking at the distribution of the crowd density, which is locally increased due to the obstacle placement. As an example, Figure 12 illustrates the distribution of the crowd density, averaged over T_{full}, for L0, L2 (LS-type) and L7 (BN-type), in the case with $\rho_{\text{m}} = 0.4$ ped/m^2: it becomes apparent that the density increase is much higher in the BN case, since the obstacle location causes a higher local reduction of the footbridge width. The main consequence of the variation in the crowd density distribution can be seen in the distribution of step frequencies. Figure 13 plots, for each layout

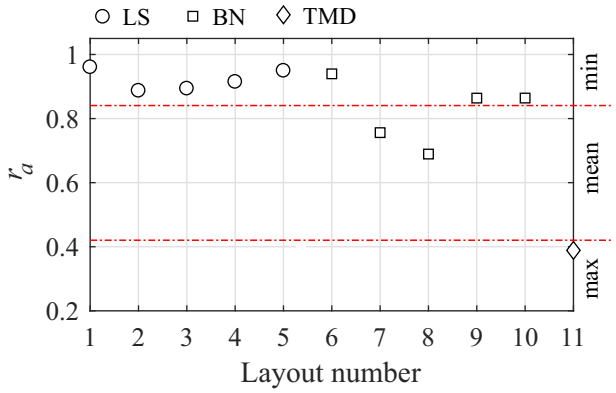

FIGURE 10 Performance index for each controlled layout, $\rho_m = 0.4$ ped/m^2

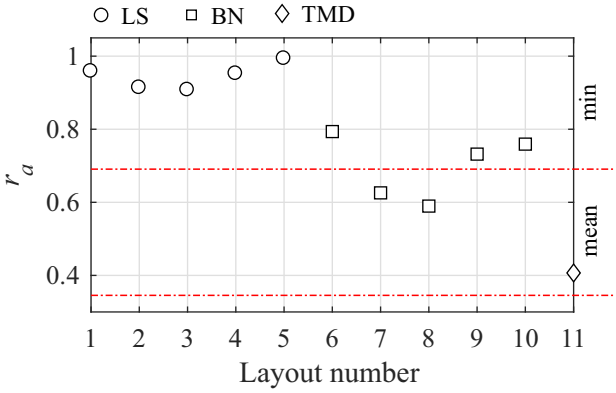

FIGURE 11 Performance index for each controlled layout, $\rho_m = 1$ ped/m^2

and $\rho_m = 0.4$ ped/m^2, the mean and std values of the step frequency. It is evident that the BN layouts are the most effective since they induce a step frequency distribution characterised by the highest dispersion and by the farthest mean value from the footbridge natural frequency f_b.

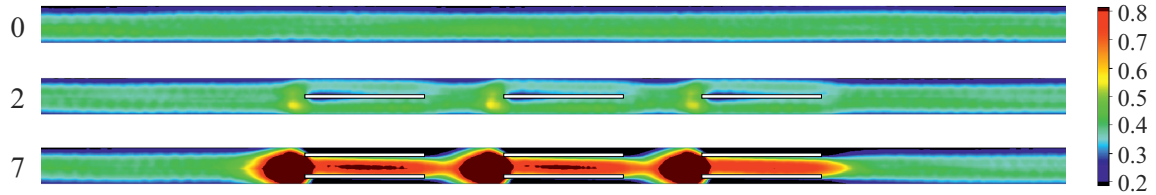

FIGURE 12 Example of the crowd density distribution averaged over T_{full} for L0, L2 and L7, $\rho_m = 0.4$ ped/m^2 (for a correct interpretation of the colors, please refer to the electronic version of the paper).

While for $\rho_m = 0.4$ and 1 ped/m^2, the crowd flow control is always effective in reducing the acceleration response (Figures 10 -11), when $\rho_m = 0.1$ ped/m^2, the average peak acceleration is higher in the majority of the controlled layouts than in the uncontrolled layout, i.e., $r_a > 1$ (Figure 9). Nevertheless, it should be observed that, in this case, the uncontrolled average peak acceleration is already in the mean comfort range and does not require mitigation. Moreover, the maximum increase in the average peak acceleration is limited to about 10% in L3.

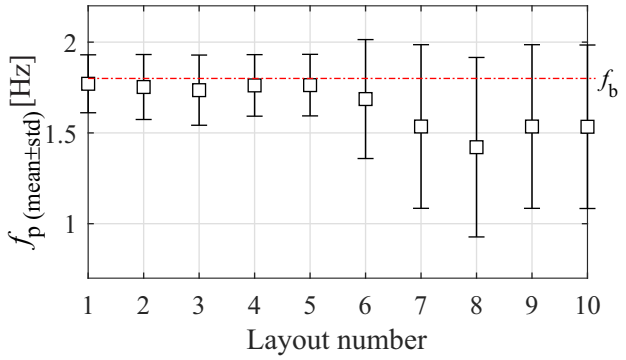

FIGURE 13 Mean and std values of the step frequency f_p for each layout with crowd flow control, $\rho_m = 0.4$ ped/m^2

Considering the footbridge provided with the installation of the optimised linear viscoelastic TMD (L11), reductions of the average peak acceleration amount to about 60% for all the considered values of crowd density. Despite the higher effectiveness of the TMD in reducing the acceleration response of the footbridge, a direct comparison with the crowd flow control is misleading, given the irreducible differences between the two mitigation strategies. First, the TMD is designed according to an optimum criterion, which is not the case of the proposed crowd flow control. Second, the two strategies have been compared only from a quantitative point of view, but other factors should be considered. In this sense, the crowd flow control presents some advantages with respect to the TMD counterpart: it can be adopted as a temporary measure, since it can be quickly installed and removed; its design, installation and maintenance costs as expected to be lower; different obstacle locations can be adopted, and changed over time, on the basis of the traffic scenario that is expected to cross the footbridge.

Finally, the robustness of the proposed crowd flow control against variations in the pedestrian excitation is evaluated by comparing its effectiveness for the different values of the mean crowd density ρ_m. Figure 14 compares the values of the average peak acceleration a_{peak} obtained in the uncontrolled layout L0, in the most effective layout with crowd flow control (L8) and in the layout with TMD (L11). Even though the TMD is always more effective in reducing the acceleration response, the performance of crowd flow control appears to be adequately robust. In particular, for mean crowd densities higher than 0.1 ped/m^2, the controlled average peak acceleration shows negligible variations (< 5%), i.e., its value remains almost constant whichever the value of the mean crowd density. This result is extremely meaningful, since it demonstrates that the proposed measure is effective even though the traffic conditions change during the footbridge lifetime.

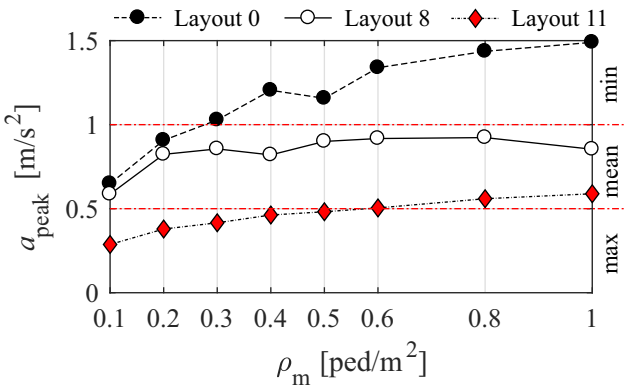

FIGURE 14 Average peak acceleration a_{peak} versus mean crowd density ρ_m in layouts L0, L8 and L11

6 | ENERGY CONSIDERATIONS

To gain a deeper insight into the principle of operation of the proposed crowd flow control, an energy formulation is developed and applied to the analysis of the dynamic response.

From an energy perspective, crowd flow control operates by modifying the characteristics of the pedestrian excitation in order to reduce the input energy transferred to the footbridge. This effect can be quantified by deriving the equation of energy balance for the generalised SDOF system: multiplying Equation 3 by velocity $\dot{y}_b(t)$ and integrating from time 0, when the dynamic excitation begins, to current time t, yields

$$E_{Kb}(t) + E_{Db}(t) + E_{Eb}(t) = E_{Ib}(t), \tag{10}$$

where $E_{Kb}(t)$ is the kinetic energy of mass M_b, $E_{Db}(t)$ is the viscous damping energy, $E_{Eb}(t)$ the elastic strain energy and $E_{Ib}(t)$ the input energy. As an example, Figure 15 illustrates the time histories of each energy contribution when the footbridge is analysed without (layout L0) and with the crowd flow control (layout L8). While $E_{Kb}(t)$ and $E_{Eb}(t)$ are functions fluctuating over time, starting from and diminishing to zero, $E_{Db}(t)$ and $E_{Ib}(t)$ converge, at the end of the structural vibration, to the same constant value, which represents the overall input energy transferred to the footbridge. From Figure 15 (d), it becomes apparent that crowd flow control greatly reduces, during the entire duration of the structural response, the input energy $E_{Ib}(t)$ entering the footbridge. In terms of maximum values, reported in Table 3 , the reduction from L0 to L8 amounts to about 40%. As a consequence, the kinetic energy and the elastic strain energy, in which the input energy converts due to the structural vibration, are also suppressed down, with reductions of more than 50% in terms of maximum values.

To comparison purposes, the energy response of the footbridge controlled via TMD is also analysed. For the generalised SDOF structure–TMD system, the equations of energy balance are derived by taking one degree of freedom at a time. Considering first

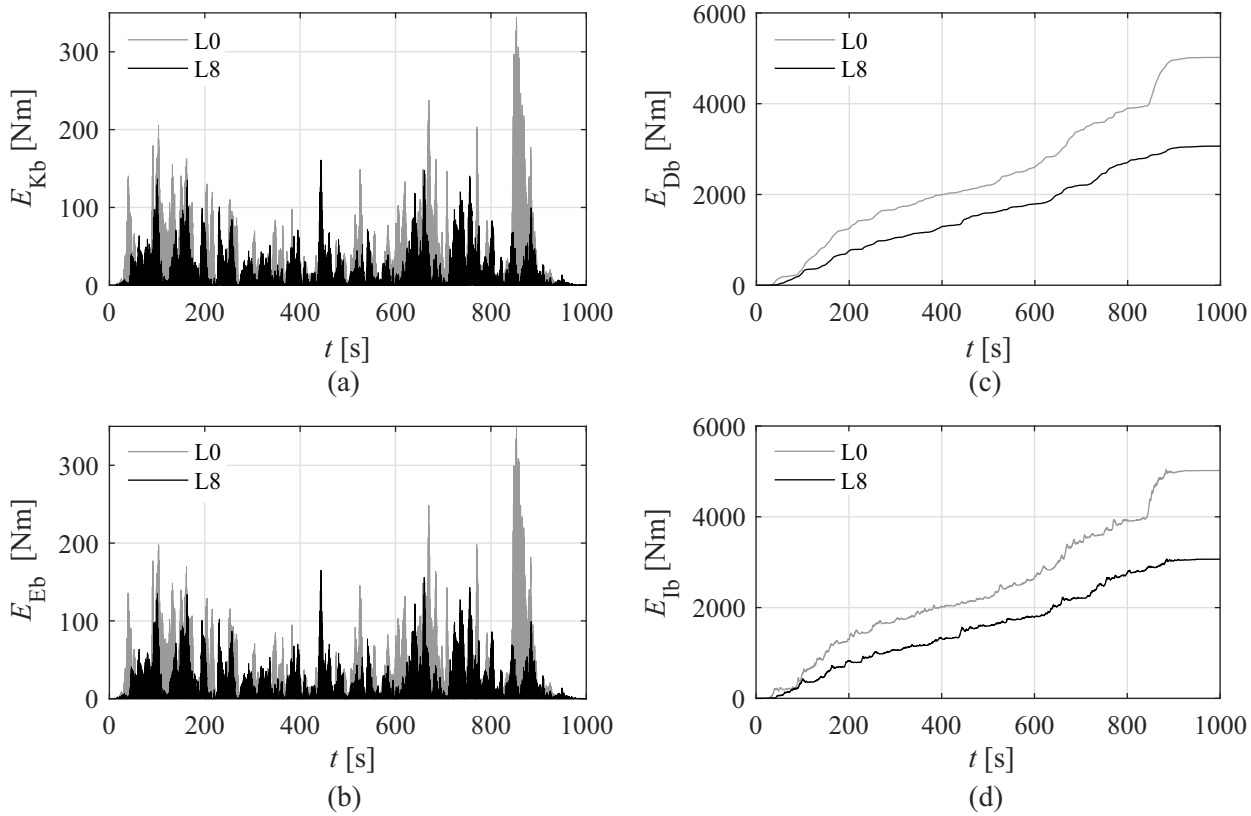

FIGURE 15 Energy response of the footbridge under pedestrian excitation with $\rho_m = 0.4$ ped/m^2, comparisons between no control (L0) and crowd flow control (L8): (a) kinetic energy E_{Kb}; (b) elastic strain energy E_{Eb}; (c) viscous damping energy E_{Db}; (d) input energy E_{Ib}.

the structure, Equation 6a is multiplied by velocity $\dot{y}_b(t)$ and integrated from time 0 to time t, yielding

$$E_{Kb}(t) + E_{Db}(t) + E_{Eb}(t) = E_{Ib}(t) - E_{FL}(t), \tag{11}$$

where $E_{Kb}(t)$, $E_{Db}(t)$, $E_{Eb}(t)$ and $E_{Ib}(t)$ are defined as in Equation 10, while

$$E_{FL}(t) = \int_0^t -u\dot{y}_b \mathrm{d}t \tag{12}$$

is the energy flowing from the structure to the TMD. The "net" input energy to the structure $E_{Ib,net}(t)$ is therefore equal to $E_{Ib}(t)$ deducted the energy flow $E_{FL}(t)$. Considering next the TMD, Equation 6b is multiplied by velocity $\dot{y}_d(t)$, rewritten in the form

$$m_d\ddot{y}_d\dot{y}_d + u\,(\dot{y}_d - \dot{y}_b) = -u\dot{y}_b \tag{13}$$

and integrating over time, obtaining

$$E_{Kd}(t) + E_{Dd}(t) + E_{Ed}(t) = E_{FL}(t), \tag{14}$$

where $E_{Kd}(t)$ is the kinetic energy of the TMD mass m_d, $E_{Dd}(t)$ is the viscous energy and $E_{Ed}(t)$ the elastic strain energy dissipated and stored, respectively, in the TMD vibration. The input energy to the TMD is represented by the energy flow $E_{FL}(t)$ from the structure.

Figure 16 illustrates the time histories of each energy contribution when the footbridge is analysed without (layout L0) and with the TMD installed (layout L11). The effect of the TMD is a significant reduction of the actual input energy to the footbridge (Figure 16 (d)): in terms of maximum values, the net input energy $E_{Ib,net}$ to the footbridge in layout L11 is equal to 12% of the input energy E_{Ib} in layout L0, as gathered from Table 3 . Such a reduction is due to the energy flow $E_{FL}(t)$ entering the

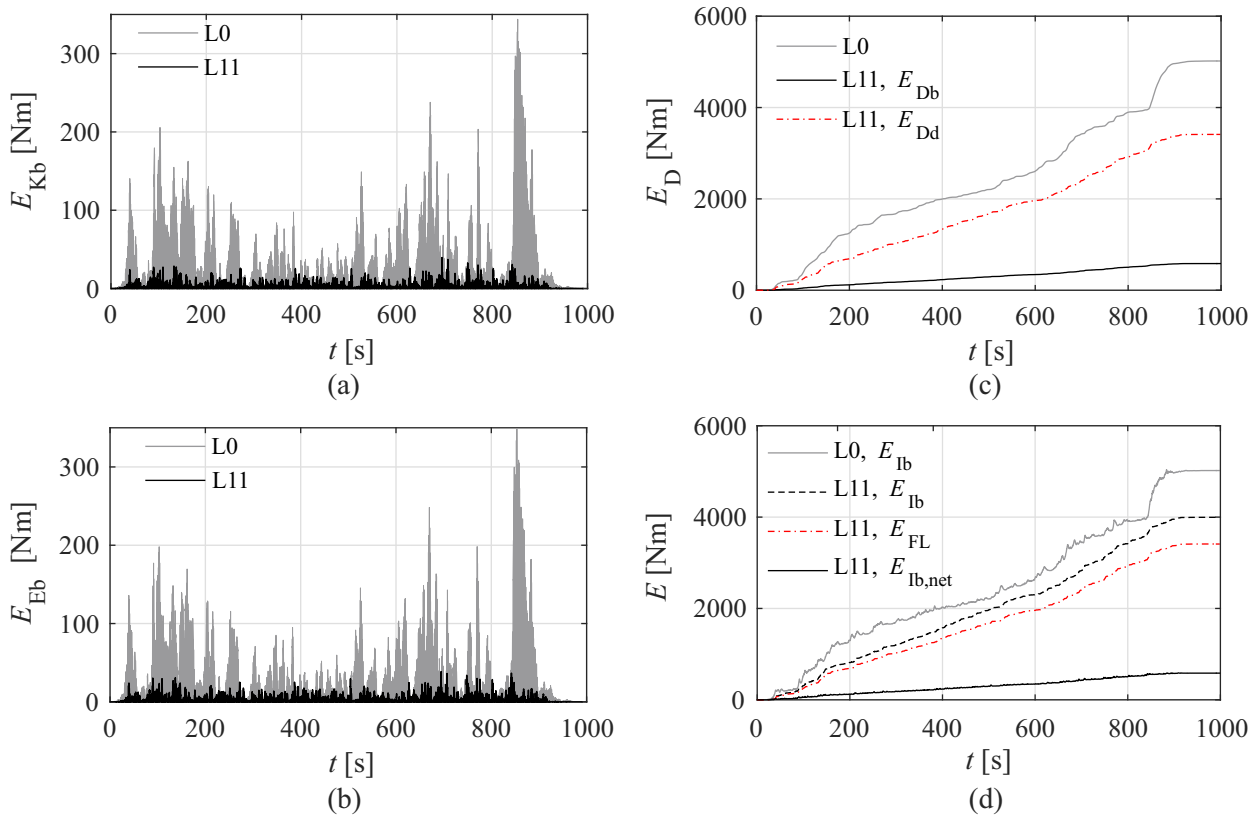

FIGURE 16 Energy response of the footbridge under pedestrian excitation with $\rho_m = 0.4$ ped/m^2, comparisons between no control (L0) and control via TMD (L11): (a) kinetic energy E_{Kb}; (b) elastic strain energy E_{Eb}; (c) viscous damping energy of the footbridge E_{Db} and of the TMD E_{Dd}; (d) input energy E_{Ib}, energy flow E_{FL} and net input energy $E_{Ib,net}$.

TMD. The TMD is hence, also called to provide supplemental viscous damping energy $E_{Dd}(t)$ in order to dissipate $E_{FL}(t)$ away (Figure 16 (c)).

TABLE 3 Maximum values of the footbridge energy response under pedestrian excitation with $\rho_m = 0.4$ ped/m^2: comparisons among no control (L0), crowd flow control (L8) and TMD (L11)

	max E_{Kb} [Nm]	max E_{Eb} [Nm]	max E_{Db} [Nm]	max E_{Ib} [Nm]
L0	343.9	348.9	5019.2	5038.3
L8	160.8	165.0	3065.6	3069.0
L11	39.6	38.6	583.9	589.6*

*Maximum value of net input energy $E_{Ib,net}$

7 | CONCLUSIONS

In this paper, a novel strategy for the mitigation of the human-induced vertical vibrations of footbridges has been proposed and explored. Aiming at acting on the source of excitation, instead of introducing modifications into the structure, the strategy is based on the crowd flow control by means of obstacles located along the footbridge span.

Crowd flow control has been applied to an ideal footbridge crossed by unidirectional traffic and subject to uncomfortable vertical vibrations under human loading. Different obstacle locations have been investigated, in order to determine the most effective one in reducing the peak vertical acceleration of the footbridge. The maximum reduction, amounting to 31%, has been obtained when the obstacles are placed to create local bottlenecks along the footbridge. A local reduction of the footbridge width results in a local increase of the crowd density and in a consequent step frequency distribution characterised a higher dispersion and farther mean value from the footbridge natural frequency f_b.

The control performance obtained through the crowd flow control has been measured against the one achieved by way of an optimised linear viscoelastic TMD, which is a structure-based mitigation strategy widespread, nowadays, in pedestrian bridges. Although the effectiveness of the TMD is higher, it has to be noted that a mere quantitative comparison in terms of control performance may be misleading, given the irreducible differences, as to design, installation and maintenance costs, between the two mitigation strategies. Moreover, the crowd flow control can be designed not only as a permanent solution (e.g., through the installation of benches or light poles) but also, more interestingly, as an emergency temporary measure (e.g., through the placement of Jersey barriers).

The results obtained from the present study have demonstrated that crowd flow control has a high potential as an effective and robust vibration mitigation strategy for footbridges and is worth further investigations. Future research will deal with the consideration of HSI in estimating the structural response and will tackle the accurate modelling of the local crowd density increase, with reference to possible congestions and delays in the crossing time.

ACKNOWLEDGEMENTS

The authors wish to thank Oasys Ltd, for having provided free licences of the software Mass Motion for academic use, and Politecnico di Torino, for the financial support received in the form of Starting Grant for Young Researchers (grants 59_ATEN_RSG17VEF and 57_ATEN_RSG16REGANN).

References

[1] 2006: *Passerelles piétonnes. Évaluation du comportement vibratoire sous l'action des piétons. (Footbridges. Assessment of vibrational behaviour of footbridges under pedestrian loading)*. Sétra/AFGC.

[2] 2017: *Mass Motion Help*. Oasys Ltd.

[3] Bachmann, H. and W. Ammann, 1987: Vibration in structures induced by man and machines. *Structural Engineering Documents*, IABSE, Zurich, volume 3a.

[4] Bocian, M., J. Brownjohn, V. Racic, D. Hester, A. Quattrone, and R. Monnickendam, 2016: A framework for experimental determination of localised vertical pedestrian forces on full-scale structures using wireless attitude and heading reference systems. *Journal of Sound and Vibration*, **376**, 217–243.

[5] Brownjohn, J., P. Fok, M. Roche, and P. Omenzetter, 2004: Long span steel pedestrian bridge at Singapore Changi Airport - Part 2: crowd loading tests and vibration mitigation measures. *The Structural Engineer*, **82**, no. 16, 21–27.

[6] Buchmueller, S. and U. Weidmann, 2006: Parameters of pedestrians, pedestrian traffic and walking facilities. n. 132. ETH. Zürich.

[7] Butz, C., M. Feldmann, C. Heinemeyer, G. Sedlacek, B. Chabrolin, A. Lemaire, M. Lukic, P. O. Martin, E. Caetano, A. Cunha, A. Goldack, A. Keil, and M. Schlaich, 2008: Advanced load models for synchronous pedestrian excitation and optimised design guidelines for steel footbridges (SYNPEX). RFS-CR 03019. Research Fund for Coal and Steel.

[8] Caetano, E., A. Cunha, F. Magalhaes, and C. Moutinho, 2010: Studies for controlling human-induced vibration of the Pedro e Inês footbridge, Portugal. Part 2: Implementation of tuned mass dampers. *Engineering Structures*, **32**, 1082–1091.

[9] Carroll, S. P., J. S. Owen, and M. F. M. Hussein, 2012: Modelling crowd-bridge dynamic interaction with a discretely defined crowd. *Journal of Sound and Vibration*, **331**, 2685–2709.

[10] Casado, C., I. Díaz, J. D. Sebastián, A. Poncela, and A. Lorenzana, 2013: Implementation of passive and active vibration control on an in-service footbridge. *Structural Control and Health Monitoring*, **20**, no. 1, 70–87.

[11] Casciati, F., S. Casciati, and L. Faravelli, 2017: A contribution to the modelling of human induced excitation on pedestrian bridges. *Structural Safety*, **66**, 51–61.

[12] da Silva, F., H. Brito, and R. Pimentel, 2014: Modeling of crowd load in vertical direction using biodynamic model for pedestrians crossing footbridges. *Canadian Journal of Civil Engineering*, **41**, 1196–1204.

[13] Dallard, P., T. Fitzpatrick, A. Flint, A. Law, R. M. Ridsdill Smith, M. Willford, and M. Roche, 2001: The London Millennium Bridge: pedestrian-induced lateral vibration. *Journal of bridge Engineering*, **6**, no. 6, 412–417.

[14] De Angelis, M., S. Perno, and A. Reggio, 2012: Dynamic response and optimal design of structures with large mass ratio TMD. *Earthquake Engineering and Structural Dynamics*, **41**, 41–60.

[15] Dziuba, P., G. Grillaud, O. Flamand, S. Sanquier, and Y. Tetard, 2001: La passerelle Solferino: comportement dynamique (Dynamic behaviour of the Solferino bridge). *Bulletin Ouvrages métalliques*, **1**, 34–57.

[16] Forner Cordero, A., H. Koopman, and F. van der Helm, 2004: Use of pressure insoles to calculate the complete ground reaction forces. *Journal of Biomechanics*, **37**, 1427–1432.

[17] He, W. and W.-P. Xie, 2018: Characterization of stationary and walking people on vertical dynamic properties of a lively lightweight bridge. *Structural Control and Health Monitoring*, **25**, no. 3, 1–24.

[18] Helbing, D., L. Buzna, A. Johansson, and T. Werner, 2005: Self-organized pedestrian crowd dynamics: Experiments, simulations and design solutions. *Transportation Science*, **39**, 1–24.

[19] Helbing, D., I. J. Farkas, P. Molnar, and T. Vicsek, 2002: Simulation of pedestrian crowds in normal and evacuation situations. *Pedestrian and Evacuation Dynamics*, M. Schreckenberg and S. D. Sharma, Eds., Springer, Berlin, 21–58.

[20] Helbing, D. and P. Molnár, 1995: Social force model for pedestrian dynamics. *Physical Review E*, **51**, no. 5, 4282–4286.

[21] Housner, G., L. Bergman, T. Caughey, A. Chassiakos, R. Claus, S. Masri, R. Skelton, T. Soong, B. Spencer, and J. Yao, 1997: Structural control: Past, present and future. *Journal of Engineering Mechanics*, **123**, no. 9, 897–971.

[22] Ingólfsson, E., C. Georgakis, R. Ricciardelli, and J. Jönsson, 2011: Experimental identification of pedestrian-induced lateral forces on footbridges. *Journal of Sound and Vibration*, **330**, 1265–1284.

[23] Kareem, A. and T. Kijewski, 1999: Mitigation of motions of tall buildings with specific examples of recent applications. *Wind and Structures*, **3**, no. 2, 201–251.

[24] Kram, R., 1998: Force treadmill for measuring vertical and horizontal ground reaction forces. *Journal of Applied Physiology*, **85**, 764–769.

[25] Law, S. S., Z. M. Wu, and S. L. Chan, 2004: Vibration control study of a suspension footbridge using hybrid slotted bolted connection elements. *Engineering Structures*, **26**, 107–116.

[26] Nimmen, K. V., G. Lombaert, G. D. Roeck, and P. V. den Broeck, 2017: The impact of vertical human-structure interaction on the response of footbridges to pedestrian excitation. *Journal of Sound and Vibration*, **402**, 104 – 121.

[27] Piccardo, G. and F. Tubino, 2012: Equivalent spectral model and maximum dynamic response for the serviceability analysis of footbridges. *Engineering Structures*, **40**, 445–456.

[28] Racic, V. and J. M. W. Brownjohn, 2011: Stochastic model of near-periodic vertical loads due to human walking. *Advanced Engineering Informatics*, **25**, 259 – 275.

[29] Racic, V., A. Pavic, and J. M. W. Brownjohn, 2009: Experimental identification and analytical modelling of human walking forces: Literature review. *Journal of Sound and Vibration*, **326**, 1–49.

[30] Reggio, A. and M. De Angelis, 2015: Optimal energy-based seismic design of non-conventional Tuned Mass Damper (TMD) implemented via inter-story isolation. *Earthquake Engineering and Structural Dynamics*, **44**, 1623–1642.

[31] Sarwar, M. W. and T. Ishihara, 2010: Numerical study on suppression of vortex-induced vibrations of box girder bridge section by aerodynamic countermeasures. *Journal of Wind Engineering and Industrial Aerodynamics*, **98**, 701–711.

[32] Shahabpoor, E., A. Pavic, V. Racic, and S. Zivanovic, 2017: Effect of group walking traffic on dynamic properties of pedestrian structures. *Journal of Sound and Vibration*, **20**, no. 207-225.

[33] Soong, T. and G. Dargush, 1997: *Passive Energy Dissipation Systems in Structural Engineering*. Wiley, New York.

[34] Tubino, F., L. Carassale, and G. Piccardo, 2016: Human-induced vibrations on two lively footbridges in Milan. *Journal of Bridge Engineering*, **21**, no. 8, 1–10.

[35] Tubino, F. and G. Piccardo, 2015: Tuned mass damper optimization for the mitigation of human-induced vibrations of pedestrian bridges. *Meccanica*, **50**, 809–824.

[36] Venuti, F. and L. Bruno, 2007: An interpretative model of the pedestrian fundamental relation. *Comptes Rendus Mecanique*, **335**, 194–200.

[37] — 2009: Crowd-structure interaction in lively footbridges under synchronous lateral excitation: A literature review. *Physics of Life Reviews*, **6**, no. 3, 176–206.

[38] — 2013: Mitigation of human-induced lateral vibrations on footbridges through walkway shaping. *Engineering Structures*, **56**, 95–104.

[39] Venuti, F., V. Racic, and A. Corbetta, 2016: Modelling framework for dynamic interaction between multiple pedestrians and vertical vibrations of footbridges. *Journal of Sound and Vibration*, **379**, 245–263.

[40] Warburton, G., 1982: Optimum absorber parameters for various combinations of response and excitation parameters. *Earthquake Engineering and Structural Dynamics*, **10**, 381–401.

[41] Young, P., 2001: Improved floor vibration prediction methodologies. *Proceedings of Arup Vibration Seminar on Engineering for Structural Vibration - Current Developments in Research and Practice*, London, UK.

[42] Zivanovic, S., 2012: Benchmark footbridge for vibration serviceability assessment under vertical component of pedestrian load. *ASCE Journal of Structural Engineering*, **138**, no. 10, 1193–1202.

How to cite this article: Venuti F., A. Reggio, (2018), Mitigation of human-induced vertical vibrations of footbridges through crowd flow control, *Struct Control Hlth*, *2018;00:–*.